MCP Papers in Press. Published on July 6, 2016 as Manuscript M116.058552

HVint: A strategy for identifying novel protein-protein interactions in herpes simplex virus type 1

Authors:

Paul Ashford[*,1], Anna Hernandez[*,1,2], Todd M. Greco*[3], Anna Buch[4], Beate Sodeik[4], Ileana M. Cristea[3,†] , Kay Grünewald[2, †], Adrian Shepherd[1,†], Maya Topf[1,†]

Authors Affiliations:

[1] Institute of Structural and Molecular Biology, Birkbeck College, University of London, Malet street, London, WC1E 7HX, UK;

[2] Oxford Particle Imaging Centre, Division of Structural Biology, Wellcome Trust Centre for Human Genetics, University of Oxford, Oxford, OX3 7BN, UK;

[3] Department of Molecular Biology, Princeton University, Lewis Thomas Laboratory, Washington Road, Princeton, NJ 08544, USA;

[4] Institute of Virology, Hannover Medical School, OE 4310, Carl-Neuberg-Str. 1, D-30623, Hannover, Germany;

*Joint first co-authors

†To whom correspondence should be addressed: E-mail: m.topf@cryst.bbk.ac.uk, Tel. +44 (0)20 7079 0886; E-mail: a.shepherd@cryst.bbk.ac.uk, Tel. +44 (0)20 7631 6886; E-mail: kay@strubi.ox.ac.uk, Tel. +44 (0)1865 287817; E-mail: icristea@princeton.edu, Tel. +1 609 258 9417

Running title: New protein-protein interactions in HSV-1

1. Abbreviations

PPI – protein-protein interaction

Y2H – Yeast Two-Hybrid

Co-IP – Co-Immunoprecipitation

MS – mass spectrometry

NMR – nuclear magnetic resonance

EMDB – Electron Microscopy Data Bank

HSV-1, HHV-1 –herpes simplex virus type 1, human herpesvirus 1

GFP – Enhanced Green Fluorescent Protein

DIP – Database of Interacting Proteins

HSV-2, HHV-2 – herpes simplex virus type 2, human herpesvirus 2

VZV, HHV-3 –varicella-zoster virus, human herpesvirus 3

EBV, HHV-4 – Epstein-Barr virus, human herpesvirus 4

HCMV, HHV-5 – human cytomegalovirus, human herpesvirus 5

HHV-6 – human herpesvirus 6

HHV-7 – human herpesvirus 7

KSHV, HHV-8 –Kaposi's sarcoma-associated herpesvirus, human herpesvirus 8

NCBI – National Center for Biotechnology Information

EMBL – European Bioinformatics Institute

DDBJ –DNA Data Bank of Japan

PDB – Protein Data Bank

HMM – Hidden Markov model

PSI – Proteomics Standards Initiative

MI – molecular interactions

CVSC – capsid vertex-specific component

PFU – plaque forming unit

2. Summary

Human herpesviruses are widespread human pathogens with a remarkable impact on worldwide public health. Despite intense decades of research, the molecular details in many aspects of their function remain to be fully characterized. To unravel the details of how these viruses operate, a thorough understanding of the relationships between the involved components is key. Here, we present HVint, a novel protein-protein intra-viral interaction resource for herpes simplex virus type 1 (HSV-1) integrating data from five external sources. To assess each interaction, we used a scoring scheme that takes into consideration aspects such as the type of detection method and the number of lines of evidence. The coverage of the initial interactome was further increased using evolutionary information, by importing interactions reported for other human herpesviruses. These latter interactions constitute, therefore, computational predictions for potential novel interactions in HSV-1. An independent experimental analysis was performed to confirm a subset of our predicted interactions. This subset covers proteins that contribute to nuclear egress and primary envelopment events, including VP26, pUL31, pUL40 and the recently characterized pUL32 and pUL21. Our findings support a coordinated crosstalk between VP26 and proteins such as pUL31, pUS9 and the CSVC complex, contributing to the development of a model describing the nuclear egress and primary envelopment pathways of newly synthesized HSV-1 capsids. The results are also consistent with recent findings on the involvement of pUL32 in capsid maturation and early tegumentation events. Further, they open the door to new hypotheses on virus-specific regulators of pUS9-dependent transport. To make this repository of interactions readily accessible for the scientific community, we also developed a user-friendly and interactive web interface. Our approach demonstrates the power of computational predictions to assist in the design of targeted experiments for the discovery of novel protein-protein interactions.

3. Introduction

One important milestone towards understanding the complexity of viral infections is to unravel the interplay between viral proteins (the *intra-viral interactome*). This is particularly important for complex and large DNA viruses, such as human herpesviruses, which have the ability to express a large number of viral gene-products. For example, the genome of HSV-1 encodes for more than 75 viral proteins, and the levels of these proteins are temporally and spatially regulated during the progression of the viral infection (1). Human herpesviruses cause life-long infections and many human and animal diseases. The severity of symptoms ranges from cold sores, genital ulcers, and blisters to blindness and life-threatening conditions, including fatal encephalitis, meningitis and cancer (2, 3). Infections from herpesviruses are also a major threat to immunosuppressed patients (*e.g.* infected by human immunodeficiency virus) and have been associated with Alzheimer's disease (3, 4).

Protein interactome studies can reveal critical biological information and shed light on mechanisms underlying infectious diseases (5), supporting proteome-wide annotation (6, 7) and the development of therapeutic strategies (8, 9)**.** The current methods used for building protein-protein interaction (PPI) networks mainly rely on known interactions and sequence analysis (11–13). Recently the field has moved forward through the development of structural and functional proteomics techniques that include fluorescence microscopy and Mass Spectrometry (MS)-based approaches (6, 14–16). These techniques have helped to increase the coverage of the interactome in the context of infection. Several public repositories of PPI data exist, such as IntAct (www.ebi.ac.uk/intact/) (15). Multiple evidence lines, depending on the nature of the interaction itself and, importantly, the detection method used, can support each individual PPI. For example, evidence for PPIs can be derived from biochemical assays, such as Yeast Two-Hybrid (Y2H),

Co-Immunoprecipitation (Co-IP), *in vitro* binding assays, and protein cross-linking, which can be then analyzed by MS. PPIs can also be derived from Nuclear Magnetic Resonance (NMR), X-ray crystallography and Electron Microscopy techniques. Most resources include evidences manually extracted from the literature. Furthermore, databases that are not explicitly dedicated to storing PPI data provide additional valuable resources, such as the Protein Data Bank (PDB www.rcsb.org/) (16) and the Electron Microscopy Data Bank (EMDB www.emdatabank.org/) (17), which contain structural information. Other databases gather PPIs based on information from multiple resources (*e.g.* VirHostNet www.virhostnet.prabi.fr/, STRING-DB http://string-db.org/) (20, 21). However, constructing a PPI network from disparate sources while ensuring trustworthiness and high coverage is challenging. Experiments vary in terms of both reliability and ability to discriminate between different categories of interactions, notably direct (physical) versus indirect interactions (*e.g.* proteins belonging to the same protein complex but without direct physical contact) as well as transient versus stable interactions (22). Moreover, for many non-model organisms, the number of known PPIs remains limited, and thus there is a need to develop hypotheses about additional PPIs that are not yet supported by direct experimental evidence.

Computational prediction of PPIs (19–23) provide the opportunity to maximize the coverage of interaction networks. These predictions often rely on sequence homology or machine learning methods (24–26). Several studies have now illustrated that transferring interaction data between close homologous species (*i.e. interologues mapping* (31)) is a suitable approach to expand PPI data for a given species. Computational methods for building and analyzing PPI networks have the potential to identify novel candidates for future experimental validation, thereby saving valuable time and resources (30, 32, 33).

In this study, we created HVint, a new database for intra-viral PPIs for an important human pathogen, of herpes simplex virus type 1 (HSV-1, also known as HHV-1), and derived the associated PPI network. To accomplish this, PPIs reported for any stage of the life cycle were compiled, *i.e.* interaction data both for proteins that are incorporated within extracellular virion particles and proteins that are only expressed in infected cells has been integrated. Information on the location of these proteins within the different structural layers of the virion particle (34, 35), namely the capsid, the tegument and the viral envelope, was included in the annotation of the interactions in HVint. To further expand the HVint database, we integrated the subsets of data from existing databases for any stage of the virus "life cycle", implemented a method for scoring multiple lines of experimental evidence, and incorporated homologous interactions from the other human herpesviruses of the α-, β- and γ-herpesvirus sub-families. As a result, our network has significantly higher coverage than previous HSV-1 networks derived from existing databases (17, 18, 20, 36, 37), and it predicts novel interactions. We validated several of these predictions by affinity purification-MS using primary human fibroblasts infected with an HSV-1 virus strain expressing the small capsid protein VP26 tagged with green fluorescent protein (EGFP). Lastly, we developed a user-friendly interactive web interface, which will allow the scientific community to readily access and analyze the interaction data. Taken together, this work demonstrates the value of data integration and homology transfer in predicting previously uncovered interactions in a complex virus such as HSV-1 and in guiding future experimental work.

4. Experimental Procedures

4.1. HVint Data Integration

The PPI data compiled to generate our novel intra-viral protein interactome includes interactions

identified by a range of experimental methods drawn from multiple sources (Figures 1 and 2). First, data from four publicly available protein interaction databases, IntAct (15) (June 2015), VirHostNet 2.0 (18) (June 2015), Database of Interacting Proteins (DIP) (36) (October 2015) and BioGRID (37) (October 2015) were collected (38–47). Custom Perl scripts were used to parse the data and to select "native" interactions directly reported for HSV-1, and "homologous" interactions originally reported for any of the other human herpesviruses, *i.e.* herpes simplex virus type 2 (HSV-2, HHV-2), varicella-zoster virus (VZV, HHV-3), Epstein-Barr virus (EBV, HHV-4), human cytomegalovirus (HCMV, HHV-5), human herpesvirus 6 (HHV-6, A and B), human herpesvirus 7 (HHV-7) or Kaposi's sarcoma-associated herpesvirus (KSHV, HHV-8). The search was conducted using taxonomy identifiers (IDs) and all reported strains for each species were considered. Where possible, protein IDs, as reported in the above interaction databases, were mapped to UniProt (48) accession numbers using the UniProt ID *mapping* tool (*e.g.* DIP and BioGRID interactor IDs are from a variety of databases, including UniProt (48), NCBI RefSeq, and EMBL/GenBank/DDBJ). In addition we collected interactions derived from structural evidence provided by the Protein Data Bank (PDB) (16) (June 2015). The taxonomy browser in PDB was used to retrieve entries associated with human herpesvirus species. The resultant list was manually curated to discard entries containing a single protein, and considered both homo- and hetero-interactions between the components. Interactions obtained from this latter dataset were also classified as native (from HSV-1) or homologous (from other human herpesvirus species) interactions according to their source species.

4.2. Homology Transfer of Interactions

Interactions gathered from other human herpesvirus species were included in HVint only if for a given interaction both interacting partners in the original species could be mapped to HSV-1

strain 17^+ using the homology detection method described below. This same rationale was also applied to transfer interactions reported for any other strains of HSV-1 different from strain 17^+. Homology relationships were defined based on the results of HHblits (49) (version 2.0.16). For each of the UniProt protein IDs involved in homologous species, its FASTA sequence was retrieved and used to generate a multiple sequence alignment against the entire UniProt Hidden Markov model (HMM) database (uniprot20_2012_10) with the number of iterations set to 3. An in-house Perl script was used to extract, where possible, the highest confidence match between the query and a protein in HSV-1 (any strain). The resulting HSV-1 UniProt IDs were mapped to HSV-1 strain 17^+ (UniProt reference proteome for HSV1) via UniRef90 clusters (50) with in-house scripts.

The distribution of the experimental detection methods defining the interactions in our database is summarised in Supplementary figure 1. Y2H methods represent the largest fraction followed by co-immunoprecipitation techniques, with more than 90% of the interactions detected so far solely by Y2H experiments. However, about 50% of the interactions (213 out of 419) are supported by two or more lines of evidence.

Based on prior knowledge, interactions in the network were also classified as interactions in the extracellular virions, *i.e.* taking place in extracellular viral particles, versus other interactions occurring during the viral lifecycle based on the classification of each of the interacting partners (34) (Supplementary figure 2). All network figures were rendered using Gephi (51).

4.3. Scoring of Interaction Data

To measure the confidence of each of the interactions in HVint, we adapted a heuristic scoring method, namely MIscore (52, 53). MIscore was chosen because its effectiveness as a scoring function capable of combining diverse factors that affect the reliability of molecular interaction

data is well established (53–55). First, scores are assigned to each individual piece of evidence for a given interaction. Aspects such as the interaction detection method(s), the type of interaction (*e.g.* co-localisation or physical association) and the number of separate studies reporting the interaction, are taken into account. To this end, each evidence line is rigorously annotated with the PSI-MI ontology (56), a controlled vocabulary developed by the Proteomics Standards Initiative (PSI) (57) for the standardization of molecular interaction (MI) annotation data (example tags are, MI:009 for "protein complementation assay" and MI:0428 for "imaging technique"). Next, scores from different lines of evidence are brought together to compute a single value per interaction. A more detailed description of MIscore can be found in (53). In our study, we modified the original MIscore function. The evidence inferred from homology was scaled according to the sequence identity between HSV-1 and the corresponding homologues, as follows: given a pair of interacting sequences *A* and *B* and their HSV-1 homologues *A'* and *B'*, the original (unmodified) MIscore was multiplied by a scaling factor *s* defined as:

$$s = \{1 \text{ if } p \geq 40;\ p/40 \text{ otherwise}\}$$

where *p* is min{sequence identity between *A* and *A'*, sequence identity between *B* and *B'*}. In other words, the score was scaled according to the lowest percentage identity between either of the interacting partners with their respective homologues. Here 40% was chosen as a conservative cut-off, taking into account prior studies of homology and the conservation PPIs between related species (53). The resulting modified MIscore scores range between 0 and 1 (Supplementary figure 3).

4.4. Network Analysis

We next assessed how filtering out interactions based on MIscore cut-offs affected the network

topology by measuring how several network properties varied as interactions with a score below a certain cut-off were removed from the network. Self-interactions were not considered during this analysis, as they do not affect most of the network properties under study. We also analysed how the network changes when separating direct *vs* indirect interactions according to the PSI-MI classification.

4.5. Experimental Validation by Affinity Purification-Mass Spectrometry

We used the HSV1(17^+)blueLox-GFPVP26 strain, here denoted HSV1-GFPVP26, in which the small capsid protein VP26 has been tagged at the N-terminus with EGFP (58). As a control, we used the HSV1(17^+)blueLox-pMCMVGFP strain, here denoted HSV1-GFP, which expresses EGFP alone, under the control of the murine cytomegalovirus promoter, inserted between the UL55 and UL56 ORFs (59). The viruses were propagated, isolated, and titered in Vero cells (ATCC CCL81) grown in DMEM containing 10% FBS and 1% penicillin/streptomycin, as previously described (60, 61). Primary human foreskin fibroblast cells (HFFs) were infected with HSV-1 strains at 1 plaque forming unit per cell (pfu/cell) for fluorescence microscopy or 5 pfu/cell for immunoaffinity purification-MS studies. The immunoaffinity purifications of GFPVP26 or EGFP during productive HSV-1 infection were accomplished using magnetic beads conjugated with in-house generated rabbit anti-GFP antibodies, as previously described (60, 62). However, for the present work, the HSV-1 strain background was 17^+, and not KOS as in our previous work. Furthermore, to capture additional interactions, we selected a cell lysis/immunoisolation buffer of intermediate stringency, namely 20 mM HEPES-KOH, pH 7.4, containing 0.11 M potassium acetate, 2 mM $MgCl_2$, 0.1% Tween 20, 1 µM $ZnCl_2$, 1 µM $CaCl_2$, 0.75 % Triton X-100, 200 mM NaCl, 0.2% deoxycholate, and 1/100 v/v protease inhibitor cocktail (Sigma). The immunoaffinity purifications of GFPVP26 and GFP were each performed

in three biological replicates.

After immunoisolation of GFPVP26 and its interacting partners, the proteins were separated (~ 3 cm) by SDS-PAGE using a 4 - 12% Bis-Tris NuPAGE gel (~3 cm), then stained with Coomassie blue and cut into gel slices. Gel slices were pooled to maintain approximate equal protein amounts (based on Coomassie blue staining) and digested in-gel with trypsin, as described (60). Extracted peptides from neighboring gel fractions were pooled (N = -6 fractions), desalted using SDB-RPS StageTips (63), concentrated to near dryness, then resuspended in 10 µl of 0.1% formic acid and analyzed by nanoliquid chromatography-tandem MS (nLC-MS/MS).

Briefly, peptides (4 µl) were separated by reverse phase chromatography-nLC (Acclaim PepMap RSLC, 1.8 µm x 75 µm x 50 cm) at a flow rate of 250 nL/min over a 90 min ACN gradient from 4 – 40% mobile phase B (A, 0.1% FA; B, 97% ACN in 0.1% FA) and ionized by ESI directly into the mass spectrometer (LTQ Orbitrap Velos equipped with an EASY-Spray ion source). The mass spectrometer was operated in a data-dependent acquisition mode. Each acquisition cycle comprised a single full-scan mass spectrum (m/z = 350-1700) in the orbitrap (r = 30,000 at m/z = 400) followed by CID MS/MS of the top 15 most abundant ions, with dynamic exclusion enabled.

MS/MS fragmentation spectra were extracted and peptide spectrum matches were obtained using Proteome Discoverer (ver. 1.4)/SEQUEST (ver 1.3) by searching independently against the forward and reverse subset of the human UniProt-SwissProt database (2013-08) appended with herpesvirus sequences and common contaminants (22, 910 sequences). SEQUEST search parameters were defined as the following: full trypsin specificity, maximum of 2 missed trypsin cleavages, ion precursor mass tolerance of 10 ppm, fragment ion mass tolerance of 0.5 Da, fixed modification of cysteine carbamidomethylation, variable modifications of methionine oxidation,

and serine, threonine, and tyrosine phosphorylation. The Proteome Discoverer workflow also included the precursor ions area detector node for MS1-based label-free quantification. Database search results were analyzed in Scaffold (ver. 4.6, Proteome Software, Inc) using the LFDR algorithm and a refinement search using the X!Tandem algorithm (Beavis Informatics), which specified the following additional modifications using the same search parameters as above: deamidation of glutamine and asparagine, acetylation of protein N-termini. The global peptide and protein FDR were controlled to ≤ 1%, estimated by reverse database search matches. The MS proteomics data have been deposited to the ProteomeXchange Consortium via the PRIDE (64) partner repository with the dataset PXD003599 and 10.6019/PXD003599 identifier. Unweighted protein spectrum counts and corresponding precursor area quantitative values were exported to Excel and additional filtering of the protein identifications was performed. Briefly, protein groups with ≥ 10 spectra in at least two out of three replicates were retained. For proteins identified in both GFPVP26 and the GFP controls, the spectral count fold enrichment was calculated for each biological replicate as the ratio of the spectral counts in each GFPVP26 replicate and the averaged GFP samples. Viral proteins with an average enrichment ratio of ≥ 5-fold were retained. The Top3 precursor area method, which uses the three most intense peptides as a measure of protein concentration (65), was used to estimate the stoichiometry of viral proteins co-isolated with GFPVP26.

4.6. Fluorescence Microscopy

Primary human fibroblast cells were cultured as described above, except on glass cover slips, and infected with HSV1-GFPVP26 at a multiplicity of infection of 1 pfu/cell. At 14 hour post-infection, cells were fixed with 2% (v/v) paraformaldehyde in PBS for 15 min at room temperature and prepared for imaging as previously described (60). Nuclei were stained with

DAPI. The subcellular localization of GFPVP26 was analyzed using a confocal microscope (Leica SP5) equipped with a 100x oil-immersion lens.

4.7. Experimental Design and Statistical Rationale

The HVint database was populated with non-redundant PPI data collated from five different public resources (IntAct, VirHostNet 2.0, DIP, BioGRID and PDB). In doing so, we distinguished between two different sets of PPI data: (a) PPIs directly reported in HSV-1 and (b) PPIs reported in other human herpesviruses species. HHblits was used to establish orthology-relationships between proteins interacting in homologous human herpesviruses and HSV-1 proteins. When HSV-1 homologous proteins were detected for both interacting partners in the source species, the interaction was transferred to the HSV-1 interactome and included in the HVint database. All PPI data in HVint was scored under the MIscore scheme, a heuristic scoring method designed to capture the heterogeneity of PPI data. MIscore is computed taken into account the annotation data for a given interaction. This annotation is defined by the HUPO PSI controlled vocabulary, which has been implemented by the public database members of the IMEx consortium (56). The final normalised scores result from the weighted sum of three different terms representing (a) the number of different citations reporting the interaction, (b) the corresponding detection method(s) used and (c) the nature of the interaction (type). An earlier study compared the performance of MIscore with that of the normalised score implemented in Mentha, a large integrative database (not containing viral interactomes) with over 570,000 PPIs (66). It was tested on a benchmark of 500 high confidence human PPIs (positive dataset) and 397 non-interactions extracted from Negatome (negative dataset) (67). Around the optimal score cut-offs for each database (0.485 for MIscore, 0.343 for the Mentha score) MIscore was shown to have greater accuracy, precision and recall than the Mentha score (0.76 *vs* 0.67, 0.70 *vs* 0.66 and

0.98 *vs* 0.85, respectively) (53). Our predicted interactions transferred from other human herpesviruses were scaled down from their originally assigned MIscore according to the sequence identity of each interacting protein to its corresponding HSV-1 homologue. The resulting scores, covering any value ranging between 0 and 1 (inclusive) with higher values reflecting higher confidence in the interaction. This calibrated scale was designed to allow users to fine-tune the selection of PPI data subsets in the database, based on their research purposes.

A subset of computationally predicted interactions was selected as potential candidates for experimental validation by IP-MS. To identify this subset we studied how several parameters characterising the topology of the interactome changed when interactions scoring below a given MIscore threshold were removed from the network. The changes in network parameters were assessed in the entire range between 0 to 1 MIscore thresholds, in steps of 0.1. The IP-MS experiments isolating HSV1-GFPVP26 were performed in three biological replicates and compared against three biological IP-MS replicates of HSV1-GFP. In total 6 biological samples were subjected to GeLC-MS/MS analysis.

5. Results

5.1. HVint Interactome

The computational and experimental pipeline developed in this work (see Experimental procedures, Figure 1) resulted in a novel HVint interactome (Figure 2). The data fed into the pipeline originated from five different resources (IntAct, VirHostNet, DIP, BioGRID and PDB) (Figures 1 and 3). PPIs reported for HSV-1 and all of the other human herpes virus species currently known (herpes simplex virus type 2, varicella-zoster virus, Epstein-Barr virus, human cytomegalovirus, human herpesviruses 6 and 7, and Kaposi's sarcoma-associated herpesvirus) were collected. The latter interactions were transferred to the HSV-1 interactome only when

orthologues for both interacting partners in the source species (*e.g.* HCMV) could be found in the HSV-1 proteome. The resulting network comprises 73 nodes and 419 PPIs (including 36 self-interactions), the reliability of which was assessed with a modified MIscore function (see Methods). The confidence values for the interactions in the network range from 0.147 to 0.972. Confidence values were computed using a highly integrative and experimentally-based scoring scheme that takes into account the type of interaction and detection method used to detect the interaction, as well as the number of different studies providing support for the interaction. Interactions were divided into two different datasets according to the source species: native interactions (reported in HSV-1) and homologous interactions (transferred from another human herpes virus species). Homologous interactions (255 in total) account for ~55% of the network, hence significantly increasing the size of the network beyond that of the native network (Figure 4A). Twenty-nine interactions are present in both native and homologous PPI datasets, indicating conservation of PPIs between two or more herpesvirus species. These conserved herpesvirus PPIs involve 50 of the HSV-1 proteins, which correspond to about 70% of the HSV-1 proteome (Figure 4B). 98% (413) of these interactions were classified as "direct interaction" or "physical association" by the PSI-MI annotation, meaning the respective experimental conditions indicate that this interaction either involves direct physical contact or that or the molecules are in close proximity.

5.2. New Interactions

Predicted PPIs that so far have not been supported by experimental evidence are of particular interest, as they point to putative biological mechanisms yet to be confirmed. To investigate whether such predicted PPIs indeed exist for HSV-1, a subset of high confidence *homologous* interactions was subjected to experimental validation. This subset was selected from the

interactions in HVint having a confidence score greater than 0.4. The rationale behind this cutoff was that the initially observed topological properties of the interactome were barely altered for confidence score cut-offs in the range between 0 and 0.4 (Supplementary figure 4), but for cut-offs between 0.4 and 0.5 drastic changes in several network parameters (including clustering coefficient, centralisation, density and average node degree) were observed. This calculated MIscore threshold is consistent with previously reported estimates of optimal cut-offs for scores predictions, within the range of 0.4 to 0.5 (53). We then retained PPIs derived from homology predictions only (*i.e.* only in the homologous dataset). By definition, these homology-based PPIs have been reported for other human herpesviruses but not yet for HSV-1.

The resulting dataset, referred hereafter as *high-confidence homologous interactions subset*, comprises a total of 35 interactions (30 hetero-interactions and 5 self-interactions) among 28 different proteins (Figure 5, Supplementary table 1). 28 hetero-interactions out of the 30 are connected in a *single connected component*, *i.e.* a group of nodes in which a path can be traced for any random pair of nodes (68). These interactions involve 23 proteins that have been annotated as being involved mainly in transcription, capsid assembly and nuclear capsid egress events (Supplementary table 2). The two binary interactions outside the main graph involve the obligate hetero-dimer gH/gL, an essential component of the herpesvirus entry machinery (69), and the tegument proteins pUL7 and pUL51. The minor capsid protein pUL25 is also present in the dataset with only one self-interaction. It is worth emphasizing that these disconnected components are nevertheless connected to the rest of the network when the whole interactome is considered (*i.e.* without filtering interactions). Our HVint interactome highlighted envelope protein pUS9 to be a hub for several potential interactions. Its predicted first neighbors, including VP26, the major small capsid protein (SCP), pUL17, another minor-capsid protein that interacts

with pUL25, and the inner tegument protein pUL36, that are known to function in capsid structure, maturation, and tegument association (70–74). As the function of these proteins has not been studied in the context of pUS9-mediated virion maturation and transport, they represent promising targets for future investigation.

5.3. *Validation of New Interactions*

To assess the informative value of our novel PPI network (Figure 5), we first searched the published literature for experimental evidence that had not been used as an input to our HVint (*i.e.* has yet to be incorporated within one of our source databases). We found recent experimental evidence supporting a complex formation of tegument proteins pUL7 and pUL51; co-immunopurification followed by MS detected this interaction, which was then confirmed and functionally characterized (75).

Second, we conducted affinity purification MS-based proteomics experiments. From the homology-based network, we selected VP26 (pUL35) for affinity purification from a productive HSV-1 infection as a respective replication-competent GFP-tagged virus was available (76). Primary human fibroblast cells were infected with HSV1-GFP or HSV1-GFPVP26, which are HSV-1 (17^{+}) strains expressing EGFP alone (control) or EGFP-tagged VP26, respectively (c.f. Experimental procedures and (76)). Wide field fluorescence microscopy was used to determine the subcellular localization of GFPVP26 following infection (Figure 6C). We focused on 14 hours post infection (p.i.), a relatively late time point in infection when under our experimental conditions capsid and virus assembly are in progress (Figure 6C). Thus, this represents the stage of infection when VP26 is predominantly nuclear, and expected to interact with other capsid components. Additionally, at this stage, capsids containing VP26 are also starting to undergo nuclear export, and thereby expected to associate with proteins involved in capsid egress. Both of

these subsets of interactions, capsid-associated and nuclear egress proteins, were part of our predicted VP26 interactions (Figure 5). The GFP tag was used for affinity isolation of GFPVP26 using specific, high-affinity anti-GFP antibodies under relatively stringent conditions (60).

The immuno-isolated proteins from cells infected with HSV1-GFP or HSV1-GFPVP26 were digested with trypsin and analyzed by liquid chromatography-tandem MS. Viral proteins detected with at least 5-fold greater spectral counts in HSV1-GFPVP26 compared to the HSV1-GFP control immuno-isolations were considered high confidence candidate interactions (Supplementary table 3). Although VP26 was isolated here using another HSV-1 strain and different lysis conditions when compared to a previous study ((60); c.f. Experimental procedures), 90% of the enriched interaction candidates were the same, pointing to reproducible findings. Importantly, our experiment confirmed two of the three predicted direct PPIs of VP26, specifically with pUL31 and pUL40 (Figure 6D, red edges). The third predicted association with pUS9 was the only predicted direct association not detected under these lysis conditions so far. However, we cannot exclude the possibility that pUS9 is a bona fide interaction that was not maintained in the applied lysis buffer. Given the relatively small size of US9 (~10 kDa and 90 amino acids), its detectability by mass spectrometry would be more challenging than either pUL31 or pUL40. In fact, an *in silico* tryptic digestion of HSV1 US9 predicts only 1 - 3 tryptic peptides to be detected under our instrument configuration and methodology.

Since immuno-affinity purification of GFPVP26 is expected to also identify indirect interacting partners, the proteins co-isolated with GFPVP26 were compared to the predicted, second order VP26 interactions (via pUL40 and pUL31, see Figure 5). Indeed, the IP-MS experimental dataset identified the proteins pUL32, pUL18, pUL26, pUL52, pUL21 and pUL10 (gM). Binary interactions between pUL40 and each of pUL32, pUL18, pUL26 and pUL52, as well as between

pUL31 and each of pUL26, pUL21 and gM are predicted by our high-confidence homologous HVint sub-network (MIscore > 0.4). Additionally, the interaction between pUL31, a nuclear egress protein, and pUL32, a protein suggested to contribute in efficient localization of newly synthesized capsids to nuclear replication compartments and DNA packaging, is present in our homology-transferred dataset but with scores below the 0.4 cut-off. Overall, the experimental immuno-affinity purification experiments provide compelling support for the homologous HVint network.

5.4. *Interactive Web-based HVint Interface*

All the data in HVint, including pairwise interactions, lines of evidence, and scores, are available for download in a standard format for molecular interactions data, namely PSI-MITAB 2.5. Additionally, we provide a user-friendly and intuitive interface to browse the data in a more straightforward and intuitive manner (http://topf-group.ismb.lon.ac.uk/hvint). The HVint interface displays an interactive graphical representation of the network and allows easy access to annotation data for individual nodes and edges. These can be selected by clicking on them or, in the case of nodes, specifying their UniProt ID in the provided search tool. The subnetwork created by the first neighbors of the selected element is then presented, together with its associated data (including a list of interactions, confidence scores and supporting evidence) in tabular form. Other functionality of the interface includes the ability to filter interactions based on user-defined confidence thresholds.

6. Discussion

HVint was originally populated with data from five major external public resources. Although some overlap exists in the data coming from these databases, each contributes multiple unique interactions. A recurrent issue in interactomics studies is the lack of network coverage, which

severely limits the informative power of the resulting networks (77, 78). Therefore, in retrieving data from the five resources, we distinguished between two datasets. One dataset contained native interactions reported as directly detected for HSV-1, and the second one was composed of homologous interactions detected in any of the other human herpesvirus species, covering all three herpesvirus sub-families. The latter dataset was then used to predict PPIs in HSV-1 based on orthology relationships between the interacting partners in the homologous species and HSV-1 proteins. Integrating these data increased the network coverage by more than two-fold. More importantly, it provides a set of putative novel interactions to be validated in HSV-1. To provide a measure of the quality and reliability of the data in the database, we implemented the MIscore (53) scoring function in our protocol. MIscore integrates data from multiple experiments that report a given interaction to calculate an overall confidence score, which is normalized to the interval [0,1]. It calculates weighted scores based on key variables: experimental detection method(s) (*e.g.* biophysical, imaging), type of interaction (*e.g.* physical association, co-localisation), and number of different scientific publications reporting it. In our implementation we gave lower weighting to orthology-transferred interactions by penalizing their original score in a sequence-identity dependent manner. An advantage of implementing this scoring scheme was that it yielded a calibrated series of scores (ranging from 0 to 1), which allowed for fine-tuned selection of sets of interactions based on their confidence levels. We used this approach to select a subset of high-confidence interactions for further experimental testing.

Overall, our interactome, including 419 interactions, achieved a notably larger coverage than any individual source database alone. This set is split between 195 native and 255 homologuous interactions, with a small subset of them overlapping between the two (31 interactions), and it covers all 77 proteins in the HSV-1 reference proteome (as reported in UniProt (48)). The data

integration framework used in this study (Figure 1) is automated and relatively simple, which will allow future updates to be implemented easily as new interaction data becomes available.

The prevalence of Y2H experiments in protein-protein interaction studies (79) is reflected in the large fraction of interactions obtained by this method in HVint (~90%, 380 interactions). This is due to the ability of Y2H experiments to determine physical pairwise interactions between potentially interacting partners, and from the feasibility of conducting both small- and large-scale screenings. Since the publication of the first large-scale protein interactions map for *S. cerevisiae* in 2000 (80), multiple studies have followed and several caveats have been raised regarding the interpretation and reliability of Y2H data, especially when obtained from high-throughput screenings (81). The main concern is the larger false positive and false negative rates than in previous traditional small-scale approaches. This has demanded a continued optimization of the technique (as shown in recent reports (79, 81–83)), and the development of a range of alternative hybrid strategies to complement Y2H datasets (79). These approaches have minimized the error rate in more recent data, suggesting that in the future the reliability of Y2H data could be assessed on a per-dataset basis in the future. HVint includes data derived from Y2H experiments across a broad period of time. Consequently, we could not yet, at present, systematically assess the quality of each dataset (as this is not reflected in the source databases). The use of MIscore as a scoring method is advantageous in this respect; it assigns comparatively low scores to interactions detected by Y2H experiments, thereby representing a conservative approach in assessing the confidence of these interactions.

To test the predictive power of our computationally derived interaction dataset, we subjected a subset of PPIs with high-confidence scores to experimental validation. To this end, a number of homologous-only interactions that scored above 0.4 were selected. We focused our own

validation analysis on VP26 (encoded by UL35), since it is a protein whose functions are still unclear, and since several HSV-1 strains in the F, 17^+ and KOS background have been generated, in which VP26 has been successfully tagged with fluorescent proteins without or with minor impairment of HSV-1 propagation (58, 60, 84–87). Hexamers of VP26 are located on top of the capsid hexons, which are hexamers of VP5, but not on the pentons, which are pentamers of VP5. VP26 is therefore perfectly placed on the capsid surface for interactions with other viral and cellular components (74, 76, 88, 89). Mutants of pseudorabies virus (PRV), a porcine α-herpesvirus, or of HSV-1, that lack VP26, are less neuroinvasive and neurovirulent and grow to lower titers than their respective parental strains (85, 90–92). VP26 can interact with the dynein light chains of the Tctex family in Y2H and coIP experiments. However, it is not required for efficient dynein-mediated transport towards the nucleus during cell entry, and dynein does not bind to un-tegumented capsids that expose VP26 over their entire surface (74, 76, 84, 93). Homologous small capsid proteins of other herpesviruses have been shown to contribute to capsid stability (94, 95).

Our HVint homologous subnetwork predicts that VP26 is associated with pUL31 and pUL40 (Figure 7). This is supported by our experimental immuno-affinity isolation studies. VP26 is present in the mature virion particle, whereas pUL31 and pUL40 are not part of it (34, 88, 89, 96–99). Hence these interactions may be particularly relevant in understanding the role of VP26 in the viral life cycle. Notably, VP26 was also co-isolated with pUL34, one of the known binding partners of pUL31 (Supplementary table 3). Together, pUL31 and pUL34 form the so-called nuclear egress complex, which is anchored to the inner nuclear membrane by the C-terminal domain of pUL34 and faces the nuclear lumen (99, 100). Given the conservation of the interaction between pUL31 and pUL34 and their respective orthologues across the entire

Herpesviridae family (101), many studies have explored their roles in the early steps of the capsid assembly and the nuclear egress pathway. Besides being recruited directly to pUL34 at the inner nuclear envelope, pUL31 has also been reported to interact via its N-terminal domain to newly synthesized nuclear capsids (102). The pUL31-bound capsids are then thought to be translocated to the inner nuclear membrane, where they associate via UL31 with pUL34 to mediate capsid egress from the nucleoplasm to the cytosol (102). Overall, the localization of VP26 to the capsid surface except the vertices, its documented roles in capsid trafficking, and our computational and experimental findings of VP26 association with nuclear egress and CVSC complexes, suggests an as yet unknown role for VP26 in enforcing capsid stability and coordinating intra-nuclear capsid trafficking events (Figure 7). Further, the recent *in situ* analyses of the NEC architecture revealed a curved hexagonal lattice for PRV (103, 104). As pUL31 and pUL34 are highly conserved in the *Herpesviridae* this architecture is highly likely to be evident in HSV-1 as well. Therefore, an attractive hypothesis is that VP26 hexamers and pUL31/34 hexamers interact directly with each other. Future, *in situ* analysis will need to show whether this is in fact the case.

Another pair of viral proteins, pUL39 and pUL40, which constitute the small and the large subunits (RR1 and RR2, respectively) of the heterotetrameric HSV-1 ribonucleotide reductase complex (105–108), were also co-isolated with VP26 by IP-MS analysis. Intriguingly, the latter was also predicted to interact with VP26 in our homologous sub-network. In addition to this enzymatic function, several studies have highlighted a role for pUL39 as a virulence factor (106, 108–110), for instance by interfering with apoptotic cascades (106, 109–111). This again suggests a potential role for VP26 in the early events of virus replication. Our experimental validation supports the interaction between VP26 via pUL40 to pUL39 and further to each of

pUL32, pUL18 (VP23) and one or more products of the HSV-1 UL26 gene, which encodes for an autocatalytic protease that is processed into the scaffold proteins VP24 and VP21 (112, 113). Notably, all these interactions have been predicted in our homologous subnetwork. Further, a recent study has provided new insights into a possible role of pUL32 as a chaperone-like protein capable of modulating capsid maturation and tegument acquisition by interacting with the capsid proteins pUL6 (the portal protein), pUL25, and pUL38 (VP19c) as well as the inner tegument protein pUL36) (114).

Amongst the membrane proteins, our HVint interactome provides a particularly high number of novel interactions for pUS9. pUS9 is a small type II membrane protein of about 10 kDa that localizes to the trans-Golgi network and axonal vesicles of neuronal cells (115–117). Our HSV-1 interactome predicts interactions between pUS9 and the capsid proteins VP26 and pUL17, as well as the inner-tegument protein pUL36. pUL17 and pUL25 form the Capsid Vertex-specific component (CVSC) located on the pentons edges and pUL17 and pUL25 are both required for stable DNA packaging into capsids prior to nuclear egress (70, 118, 119). pUL36 is an inner protein known to be involved in early tegumentation events together with its binding partner pUL37 (72, 84). Like the CVSC, the complex pUL36-pUL37 is also located around penton vertices. Interestingly, PPIs and coordinated events between pUL36-pUL37 and CVSC have been previously shown (72). Together with the heterodimer gE/gI, pUS9 mediates anterograde axonal transport of viral tegument, glycoproteins and virions of α-herpesviruses in neurons, but these proteins are not essential for replication in epithelial or fibroblasts cells (40–42). While studies on the gE/gI and pUS9-mediated transport of PRV structures show that PRV is transported along axons as fully assembled virions in transport vesicles, the data on HSV-1 regarding the sub-viral and viral particles being targeted to axons is still controversial (116, 117,

120). Since the HSV-1 or PRV proteins that might contribute to these differences are not known, our novel predicted interactions from HVint generate new hypotheses on potentially virus-specific regulators of US9-dependent anterograde transport.

The nodes outside the main cluster of the 35 new interactions involve those forming two heterodimers conserved across the entire *Herpesviridae* family, namely gH/gL and pUL51-pUL7, and one self-interaction for pUL25. The complex gH/gL was structurally solved in HSV-2 by X-ray crystallography in 2010 (121). Given the high confidence of the experimental data and the degree of sequence similarity between HSV-1 and HSV-2 gH/gL sequences, the existence of this complex in HSV-1 is undisputed (121–123). Although its specific role is yet to be fully defined, it is likely involved in regulating the activity of the membrane fusion glycoprotein gB (121).

Finally, complex formation between pUL51 and pUL7, as predicted in our HVint database, was confirmed recently by affinity purification and tandem MS experiments (75). At the time of writing, these data were not integrated, to the source PPI databases used in this work. pUL51 and pUL7 are both conserved across the whole *Herpesviridae* family. pUL51 is an N-terminus membrane-anchored tegument protein (124–126) with no apparent enzymatic function, suggested to play a role in viral egress, viral envelopment and epithelial cell-to-cell spread (127, 128). Its interaction with pUL7 seems to be required for efficient recruitment of the latter to cytoplasmic membranes leading to its incorporation into the virion. Both proteins partially co-localize in cytoplasmic membranes together, as observed in the case of pUS9, with glycoprotein gE (128). This implies that the complex is non-obligate and each protein could carry out independent functional activities. pUL7 was also found inside the nuclear and cytoplasmic compartments in the absence of pUL51, and interactions between pUL7 and capsid proteins have been reported. As in the case of pUS9, the complex between pUL51 and pUL7 supports the idea

that viral membrane proteins are principal agents in tegumentation and secondary envelopment processes. By establishing interactions with capsid and capsid-associated proteins they guide progeny virion particles to different cytoplasmic compartments (*e.g.* trans Golgi network or endosomes) until they reach the plasma membrane (42, 129–134).

7. Conclusions

Here we introduce the HVint database, an integrative resource for HSV-1 molecular interaction data. The database contains interactions experimentally detected in HSV-1 species and computationally predicted using evolutionary information. Interactions in the database have been scored, thus confidently providing novel predicted interactions. Consequently, HVint can be used as a tool to prioritize candidate interactions for future experimental testing. The protocol used to create and populate the database was kept simple, hence facilitating database updates. In the future, our aim is to further improve our methods for assessing the reliability of molecular interaction data and to include more advanced features in the HVint graphical interface to accommodate users' needs. We also plan to extend the current database to other human herpesvirus species and to virus-host interactions.

8. Acknowledgements

We thank Dr. David Houldershaw for computer support. We thank Drs. Tzviya Zeev-Ben-Mordehai and Daven Vasishtan for helpful discussions. We thank Ben Diner, Marni Crow, and Minghao Li for technical assistance with control isolations. The work was supported by the MRC [G0600084] (M.T.) and [MR/M019292/1] (M.T., K.G.), the Leverhulme Trust [RPG-2012-519] (M.T., K.G.), the Niedersachsen Research Network on Neuroinfectiology (NRENNT) of the Ministry of Science and Culture of Lower Saxony, Germany (A.B., B.S.), the Wellcome Trust [090895/Z/09/Z, 090532/Z/09/Z, 107806/Z/15/Z,] (K.G.), the HFSP [RGY0079/2009-C] (K.G., M.T., I.C.], and grants from the National Institutes of Health (AI102187 and GM114141) (I.M.C), NJCCR fellowship to T.M.G.

9. References

1. Engel, E. A., Song, R., Koyuncu, O. O., and Enquist, L. W. (2015) Investigating the biology of alpha herpesviruses with MS-based proteomics. *Proteomics* 15, 1943–56
2. Brady, R. C., and Bernstein, D. I. (2004) Treatment of herpes simplex virus infections. *Antiviral Res* 61, 73–81
3. Chentoufi, A. A., and Benmohamed, L. (2012) Mucosal herpes immunity and immunopathology to ocular and genital herpes simplex virus infections. *Clin Dev Immunol* 2012, 149135
4. Lövheim, H., Gilthorpe, J., Adolfsson, R., Nilsson, L. G., and Elgh, F. (2014) Reactivated herpes simplex infection increases the risk of Alzheimer's disease. *Alzheimers Dement* 11, 593–9
5. Rollenhagen, C., Lathrop, M. J., Macura, S. L., Doncel, G. F., and Asin, S. N. (2014) Herpes simplex virus type-2 stimulates HIV-1 replication in cervical tissues: implications for HIV-1 transmission and efficacy of anti-HIV-1 microbicides. *Mucosal Immunol* 7, 1165–74
6. Marcoux, J., and Cianférani, S. (2015) Towards integrative structural mass spectrometry: Benefits from hybrid approaches. *Methods* 89, 4–12
7. Stelzl, U., Worm, U., Lalowski, M., Haenig, C., Brembeck, F. H., Goehler, H., Stroedicke, M., Zenkner, M., Schoenherr, A., Koeppen, S., Timm, J., Mintzlaff, S., Abraham, C., Bock, N., Kietzmann, S., Goedde, A., Toksöz, E., Droege, A., Krobitsch, S., Korn, B., Birchmeier, W., Lehrach, H., and Wanker, E. E. (2005) A human protein-protein interaction network: A resource for annotating the proteome. *Cell* 122, 957–968
8. Deng, M., Zhang, K., Mehta, S., Chen, T., and Sun, F. (2002) Prediction of protein

function using protein-protein interaction data. *Proc IEEE Comput Soc Bioinform Conf* 1, 197–206

9. Jaeger, S., and Aloy, P. (2012) From protein interaction networks to novel therapeutic strategies. *IUBMB Life* 64, 529–37
10. de Chassey, B., Meyniel-Schicklin, L., Vonderscher, J., André, P., and Lotteau, V. (2014) Virus-host interactomics: new insights and opportunities for antiviral drug discovery. *Genome Med* 6, 115
11. Nourani, E., Khunjush, F., and Durmuş, S. (2015) Computational approaches for prediction of pathogen-host protein-protein interactions. *Front Microbiol* 6, 94
12. Kshirsagar, M., Carbonell, J., and Klein-Seetharaman, J. (2012) Techniques to cope with missing data in host-pathogen protein interaction prediction. *Bioinformatics* 28, i466–i472
13. Durmuş Tekir, S. D., and Ülgen, K. Ö. (2013) Systems biology of pathogen-host interaction: Networks of protein-protein interaction within pathogens and pathogen-human interactions in the post-genomic era. *Biotechnol J* 8, 85–96
14. Greco, T. M., Diner, B. A., and Cristea, I. M. (2014) The Impact of Mass Spectrometry–Based Proteomics on Fundamental Discoveries in Virology. *Annu Rev Virol* 1, 581–604
15. DeBlasio, S. L., Chavez, J. D., Alexander, M. M., Ramsey, J., Eng, J. K., Mahoney, J., Gray, S. M., Bruce, J. E., and Cilia, M. (2015) Visualization of host-polerovirus interaction topologies using Protein Interaction Reporter technology. *J Virol* 90, 1973–87
16. Ramisetty, S. R., and Washburn, M. P. (2011) Unraveling the dynamics of protein interactions with quantitative mass spectrometry. *Crit Rev Biochem Mol Biol* 46, 216–28
17. Orchard, S., Ammari, M., Aranda, B., Breuza, L., Briganti, L., Broackes-Carter, F., Campbell, N. H., Chavali, G., Chen, C., Del-Toro, N., Duesbury, M., Dumousseau, M.,

Galeota, E., Hinz, U., Iannuccelli, M., Jagannathan, S., Jimenez, R., Khadake, J., Lagreid, A., Licata, L., Lovering, R. C., Meldal, B., Melidoni, A. N., Milagros, M., Peluso, D., Perfetto, L., Porras, P., Raghunath, A., Ricard-Blum, S., Roechert, B., Stutz, A., Tognolli, M., van Roey, K., Cesareni, G., and Hermjakob, H. (2014) The MIntAct project - IntAct as a common curation platform for 11 molecular interaction databases. *Nucleic Acids Res* 42, D358–63

18. Berman, H. M. (2000) The Protein Data Bank. *Nucleic Acids Res* 28, 235–242
19. Lawson, C. L., Baker, M. L., Best, C., Bi, C., Dougherty, M., Feng, P., van Ginkel, G., Devkota, B., Lagerstedt, I., Ludtke, S. J., Newman, R. H., Oldfield, T. J., Rees, I., Sahni, G., Sala, R., Velankar, S., Warren, J., Westbrook, J. D., Henrick, K., Kleywegt, G. J., Berman, H. M., and Chiu, W. (2011) EMDataBank.org: unified data resource for CryoEM. *Nucleic Acids Res* 39, D456–64
20. Guirimand, T., Delmotte, S., and Navratil, V. (2015) VirHostNet 2.0: surfing on the web of virus/host molecular interactions data. *Nucleic Acids Res* 43, D583–7
21. Szklarczyk, D., Franceschini, A., Wyder, S., Forslund, K., Heller, D., Huerta-Cepas, J., Simonovic, M., Roth, A., Santos, A., Tsafou, K. P., Kuhn, M., Bork, P., Jensen, L. J., and von Mering, C. (2015) STRING v10: protein-protein interaction networks, integrated over the tree of life. *Nucleic Acids Res* 43, D447–52
22. Budayeva, H. G., and Cristea, I. M. (2014) A mass spectrometry view of stable and transient protein interactions. *Adv Exp Med Biol* 806, 263–82
23. McDowall, M. D., Scott, M. S., and Barton, G. J. (2009) PIPs: human protein-protein interaction prediction database. *Nucleic Acids Res* 37, D651–6
24. Hosur, R., Peng, J., Vinayagam, A., Stelzl, U., Xu, J., Perrimon, N., Bienkowska, J., and

Berger, B. (2012) A computational framework for boosting confidence in high-throughput protein-protein interaction datasets. *Genome Biol* 13, R76

25. Zahiri, J., Bozorgmehr, J. H., and Masoudi-Nejad, A. (2013) Computational Prediction of Protein-Protein Interaction Networks: Algorithms and Resources. *Curr Genomics* 14, 397–414

26. Hosur, R., Xu, J., Bienkowska, J., and Berger, B. (2011) iWRAP: An interface threading approach with application to prediction of cancer-related protein-protein interactions. *J Mol Biol* 405, 1295–310

27. Singh, R., Park, D., Xu, J., Hosur, R., and Berger, B. (2010) Struct2Net: a web service to predict protein-protein interactions using a structure-based approach. *Nucleic Acids Res* 38, W508–15

28. You, Z. H., Chan, K. C. C., and Hu, P. (2015) Predicting protein-protein interactions from primary protein sequences using a novel multi-scale local feature representation scheme and the random forest. *PLoS One* 10, e0125811

29. Zhang, Y. N., Pan, X. Y., Huang, Y., and Shen, H. Bin (2011) Adaptive compressive learning for prediction of protein-protein interactions from primary sequence. *J Theor Biol* 283, 44–52

30. Folador, E. L., Hassan, S. S., Lemke, N., Barh, D., Silva, A., Ferreira, R. S., and Azevedo, V. (2014) An improved interolog mapping-based computational prediction of protein–protein interactions with increased network coverage. *Integr. Biol.* 6, 1080–1087

31. Yu, H., Luscombe, N. M., Lu, H. X., Zhu, X., Xia, Y., Han, J. D. J., Bertin, N., Chung, S., Vidal, M., and Gerstein, M. (2004) Annotation transfer between genomes: protein-protein interologs and protein-DNA regulogs. *Genome Res* 14, 1107–18

32. Murakami, Y., and Mizuguchi, K. (2014) Homology-based prediction of interactions between proteins using Averaged One-Dependence Estimators. *BMC Bioinformatics* 15, 213

33. Saeed, R., and Deane, C. (2008) An assessment of the uses of homologous interactions. *Bioinformatics* 24, 689–95

34. Loret, S., Guay, G., and Lippé, R. (2008) Comprehensive characterization of extracellular herpes simplex virus type 1 virions. *J Virol* 82, 8605–18

35. Grünewald, K., Desai, P., Winkler, D. C., Heymann, J. B., Belnap, D. M., Baumeister, W., and Steven, A. C. (2003) Three-dimensional structure of herpes simplex virus from cryo-electron tomography. *Science* 302, 1396–8

36. Xenarios, I., Fernandez, E., Salwinski, L., Duan, X. J., Thompson, M. J., Marcotte, E. M., and Eisenberg, D. (2001) DIP: The Database of Interacting Proteins: 2001 update. *Nucleic Acids Res* 29, 239–241

37. Chatr-Aryamontri, A., Breitkreutz, B. J., Oughtred, R., Boucher, L., Heinicke, S., Chen, D., Stark, C., Breitkreutz, A., Kolas, N., O'Donnell, L., Reguly, T., Nixon, J., Ramage, L., Winter, A., Sellam, A., Chang, C., Hirschman, J., Theesfeld, C., Rust, J., Livstone, M. S., Dolinski, K., and Tyers, M. (2015) The BioGRID interaction database: 2015 update. *Nucleic Acids Res* 43, D470–8

38. Calderwood, M. A., Venkatesan, K., Xing, L., Chase, M. R., Vazquez, A., Holthaus, A. M., Ewence, A. E., Li, N., Hirozane-Kishikawa, T., Hill, D. E., Vidal, M., Kieff, E., and Johannsen, E. (2007) Epstein-Barr virus and virus human protein interaction maps. *Proc Natl Acad Sci U S A* 104, 7606–11

39. Panagiotidis, C. A., Lium, E. K., and Silverstein, S. J. (1997) Physical and functional

interactions between herpes simplex virus immediate-early proteins ICP4 and ICP27. *J Virol* 71, 1547–57

40. Rozen, R., Sathish, N., Li, Y., and Yuan, Y. (2008) Virion-wide protein interactions of Kaposi's sarcoma-associated herpesvirus. *J Virol* 82, 4742–50

41. Taylor, T. J., and Knipe, D. M. (2004) Proteomics of herpes simplex virus replication compartments: association of cellular DNA replication, repair, recombination, and chromatin remodeling proteins with ICP8. *J Virol* 78, 5856–66

42. Vittone, V., Diefenbach, E., Triffett, D., Douglas, M. W., Cunningham, A. L., and Diefenbach, R. J. (2005) Determination of interactions between tegument proteins of herpes simplex virus type 1. *J Virol* 79, 9566–71

43. To, A., Bai, Y., Shen, A., Gong, H., Umamoto, S., Lu, S., and Liu, F. (2011) Yeast two hybrid analyses reveal novel binary interactions between human cytomegalovirus-encoded virion proteins. *PLoS One* 6, e17796

44. Lee, J. H., Vittone, V., Diefenbach, E., Cunningham, A. L., and Diefenbach, R. J. (2008) Identification of structural protein-protein interactions of herpes simplex virus type 1. *Virology* 378, 347–54

45. Uetz, P., Dong, Y. A., Zeretzke, C., Atzler, C., Baiker, A., Berger, B., Rajagopala, S. V, Roupelieva, M., Rose, D., Fossum, E., and Haas, J. (2006) Herpesviral protein networks and their interaction with the human proteome. *Science* 311, 239–42

46. Stellberger, T., Häuser, R., Baiker, A., Pothineni, V. R., Haas, J., and Uetz, P. (2010) Improving the yeast two-hybrid system with permutated fusions proteins: the Varicella Zoster Virus interactome. *Proteome Sci* 8, 8

47. Fossum, E., Friedel, C. C., Rajagopala, S. V, Titz, B., Baiker, A., Schmidt, T., Kraus, T.,

Stellberger, T., Rutenberg, C., Suthram, S., Bandyopadhyay, S., Rose, D., von Brunn, A., Uhlmann, M., Zeretzke, C., Dong, Y. A., Boulet, H., Koegl, M., Bailer, S. M., Koszinowski, U., Ideker, T., Uetz, P., Zimmer, R., and Haas, J. (2009) Evolutionarily conserved herpesviral protein interaction networks. *PLoS Pathog* 5, e1000570

48. The UniProt Consortium (2014) UniProt: a hub for protein information. *Nucleic Acids Res* 43, D204–212

49. Remmert, M., Biegert, A., Hauser, A., and Söding, J. (2012) HHblits: lightning-fast iterative protein sequence searching by HMM-HMM alignment. *Nat Methods* 9, 173–5

50. Suzek, B. E., Wang, Y., Huang, H., McGarvey, P. B., and Wu, C. H. (2015) UniRef clusters: a comprehensive and scalable alternative for improving sequence similarity searches. *Bioinformatics* 31, 926–32

51. Bastian, M., Heymann, S., and Jacomy, M. (2009) in *International AAAI Conference on Weblogs and Social Media*

52. Aranda, B., Blankenburg, H., Kerrien, S., Brinkman, F. S. L., Ceol, A., Chautard, E., Dana, J. M., De Las Rivas, J., Dumousseau, M., Galeota, E., Gaulton, A., Goll, J., Hancock, R. E. W., Isserlin, R., Jimenez, R. C., Kerssemakers, J., Khadake, J., Lynn, D. J., Michaut, M., O'Kelly, G., Ono, K., Orchard, S., Prieto, C., Razick, S., Rigina, O., Salwinski, L., Simonovic, M., Velankar, S., Winter, A., Wu, G., Bader, G. D., Cesareni, G., Donaldson, I. M., Eisenberg, D., Kleywegt, G. J., Overington, J., Ricard-Blum, S., Tyers, M., Albrecht, M., and Hermjakob, H. (2011) PSICQUIC and PSISCORE: accessing and scoring molecular interactions. *Nat Methods* 8, 528–9

53. Villaveces, J. M., Jiménez, R. C., Porras, P., Del-Toro, N., Duesbury, M., Dumousseau, M., Orchard, S., Choi, H., Ping, P., Zong, N. C., Askenazi, M., Habermann, B. H., and

Hermjakob, H. (2015) Merging and scoring molecular interactions utilising existing community standards: tools, use-cases and a case study. *Database (Oxford)* 2015, bau131

54. López-Blanco, J. R., and Chacón, P. (2015) Structural modeling from electron microscopy data. *Wiley Interdiscip Rev Comput Mol Sci* 5, 62–81

55. Mora, A., and Donaldson, I. M. (2012) Effects of protein interaction data integration, representation and reliability on the use of network properties for drug target prediction. *BMC Bioinformatics* 13, 294

56. Kerrien, S., Orchard, S., Montecchi-Palazzi, L., Aranda, B., Quinn, A. F., Vinod, N., Bader, G. D., Xenarios, I., Wojcik, J., Sherman, D., Tyers, M., Salama, J. J., Moore, S., Ceol, A., Chatr-Aryamontri, A., Oesterheld, M., Stümpflen, V., Salwinski, L., Nerothin, J., Cerami, E., Cusick, M. E., Vidal, M., Gilson, M., Armstrong, J., Woollard, P., Hogue, C., Eisenberg, D., Cesareni, G., Apweiler, R., and Hermjakob, H. (2007) Broadening the horizon--level 2.5 of the HUPO-PSI format for molecular interactions. *BMC Biol* 5, 44

57. Deutsch, E. W., Albar, J. P., Binz, P.-A., Eisenacher, M., Jones, A. R., Mayer, G., Omenn, G. S., Orchard, S., Vizcaíno, J. A., and Hermjakob, H. (2015) Development of data representation standards by the human proteome organization proteomics standards initiative. *J Am Med Inform Assoc* 22, 495–506

58. Nagel, C. H., Döhner, K., Binz, A., Bauerfeind, R., and Sodeik, B. (2012) Improper tagging of the non-essential small capsid protein VP26 impairs nuclear capsid egress of herpes simplex virus. *PLoS One* 7, e44177

59. Snijder, B., Sacher, R., Ramo, P., Liberali, P., Mench, K., Wolfrum, N., Burleigh, L., Scott, C. C., Verheije, M. H., Mercer, J., Moese, S., Heger, T., Theusner, K., Jurgeit, A., Lamparter, D., Balistreri, G., Schelhaas, M., De Haan, C. A. M., Marjomaki, V., Hyypia,

T., Rottier, P. J. M., Sodeik, B., Marsh, M., Gruenberg, J., Amara, A., Greber, U., Helenius, A., and Pelkmans, L. (2012) Single-cell analysis of population context advances RNAi screening at multiple levels. *Mol Syst Biol* 8, 579

60. Rowles, D. L., Tsai, Y. C., Greco, T. M., Lin, A. E., Li, M., Yeh, J., and Cristea, I. M. (2015) DNA methyltransferase DNMT3A associates with viral proteins and impacts HSV-1 infection. *Proteomics* 15, 1968–1982

61. Lin, A. E., Greco, T. M., Döhner, K., Sodeik, B., and Cristea, I. M. (2013) A proteomic perspective of inbuilt viral protein regulation: pUL46 tegument protein is targeted for degradation by ICP0 during herpes simplex virus type 1 infection. *Mol Cell Proteomics* 12, 3237–52

62. Cristea, I. M., Williams, R., Chait, B. T., and Rout, M. P. (2005) Fluorescent proteins as proteomic probes. *Mol Cell Proteomics* 4, 1933–41

63. Kulak, N. a, Pichler, G., Paron, I., Nagaraj, N., and Mann, M. (2014) Minimal, encapsulated proteomic-sample processing applied to copy-number estimation in eukaryotic cells. *Nat Methods* 11, 319–24

64. Vizcaíno, J. A., Csordas, A., Del-Toro, N., Dianes, J. A., Griss, J., Lavidas, I., Mayer, G., Perez-Riverol, Y., Reisinger, F., Ternent, T., Xu, Q. W., Wang, R., and Hermjakob, H. (2016) 2016 update of the PRIDE database and its related tools. *Nucleic Acids Res* 44, D447–56

65. Silva, J. C., Gorenstein, M. V, Li, G. Z., Vissers, J. P. C., and Geromanos, S. J. (2006) Absolute quantification of proteins by LCMSE: a virtue of parallel MS acquisition. *Mol Cell Proteomics* 5, 144–56

66. Calderone, A., Castagnoli, L., and Cesareni, G. (2013) mentha: a resource for browsing

integrated protein-interaction networks. *Nat Methods* 10, 690–1

67. Blohm, P., Frishman, G., Smialowski, P., Goebels, F., Wachinger, B., Ruepp, A., and Frishman, D. (2014) Negatome 2.0: a database of non-interacting proteins derived by literature mining, manual annotation and protein structure analysis. *Nucleic Acids Res* 42, D396–400

68. Winterbach, W., Van Mieghem, P., Reinders, M., Wang, H., and de Ridder, D. (2013) Topology of molecular interaction networks. *BMC Syst Biol* 7, 90

69. Connolly, S. A., Jackson, J. O., Jardetzky, T. S., and Longnecker, R. (2011) Fusing structure and function: a structural view of the herpesvirus entry machinery. *Nat Rev Microbiol* 9, 369–81

70. Toropova, K., Huffman, J. B., Homa, F. L., and Conway, J. F. (2011) The herpes simplex virus 1 UL17 protein is the second constituent of the capsid vertex-specific component required for DNA packaging and retention. *J Virol* 85, 7513–22

71. Trus, B. L., Homa, F. L., Booy, F. P., Newcomb, W. W., Thomsen, D. R., Cheng, N., Brown, J. C., and Steven, A. C. (1995) Herpes simplex virus capsids assembled in insect cells infected with recombinant baculoviruses: structural authenticity and localization of VP26. *J Virol* 69, 7362–6

72. Cardone, G., Newcomb, W. W., Cheng, N., Wingfield, P. T., Trus, B. L., Brown, J. C., and Steven, A. C. (2012) The UL36 Tegument Protein of Herpes Simplex Virus 1 Has a Composite Binding Site at the Capsid Vertices. *J Virol* 86, 4058–4064

73. Zhou, Z. H., He, J., Jakana, J., Tatman, J. D., Rixon, F. J., and Chiu, W. (1995) Assembly of VP26 in herpes simplex virus-1 inferred from structures of wild-type and recombinant capsids. *Nat Struct Biol* 2, 1026–30

74. Douglas, M. W., Diefenbach, R. J., Homa, F. L., Miranda-Saksena, M., Rixon, F. J., Vittone, V., Byth, K., and Cunningham, A. L. (2004) Herpes Simplex Virus Type 1 Capsid Protein VP26 Interacts with Dynein Light Chains RP3 and Tctex1 and Plays a Role in Retrograde Cellular Transport. *J Biol Chem* 279, 28522–28530

75. Roller, R. J., and Fetters, R. (2015) The Herpes Simplex Virus 1 UL51 Protein Interacts with the UL7 Protein and Plays a Role in Its Recruitment into the Virion. *J Virol* 89, 3112–3122

76. Döhner, K., Radtke, K., Schmidt, S., and Sodeik, B. (2006) Eclipse phase of herpes simplex virus type 1 infection: Efficient dynein-mediated capsid transport without the small capsid protein VP26. *J Virol* 80, 8211–24

77. Navlakha, S., and Kingsford, C. (2010) The power of protein interaction networks for associating genes with diseases. *Bioinformatics* 26, 1057–63

78. Marras, E., Travaglione, A., Chaurasia, G., Futschik, M., and Capobianco, E. (2010) Inferring modules from human protein interactome classes. *BMC Syst Biol* 4, 102

79. Brückner, A., Polge, C., Lentze, N., Auerbach, D., and Schlattner, U. (2009) Yeast two-hybrid, a powerful tool for systems biology. *Int J Mol Sci* 10, 2763–88

80. Uetz, P., Giot, L., Cagney, G., Mansfield, T. A., Judson, R. S., Knight, J. R., Lockshon, D., Narayan, V., Srinivasan, M., Pochart, P., Qureshi-Emili, A., Li, Y., Godwin, B., Conover, D., Kalbfleisch, T., Vijayadamodar, G., Yang, M., Johnston, M., Fields, S., and Rothberg, J. M. (2000) A comprehensive analysis of protein-protein interactions in Saccharomyces cerevisiae. *Nature* 403, 623–627

81. Grünenfelder, B., and Winzeler, E. A. (2002) Treasures and traps in genome-wide data sets: case examples from yeast. *Nat Rev Genet* 3, 653–61

82. Chen, Y. C., Rajagopala, S. V., Stellberger, T., and Uetz, P. (2010) Exhaustive benchmarking of the yeast two-hybrid system. *Nat Methods* 7, 667–8

83. Sprinzak, E., Sattath, S., and Margalit, H. (2003) How reliable are experimental protein-protein interaction data? *J Mol Biol* 327, 919–23

84. Desai, P., Sexton, G. L., Huang, E., and Person, S. (2008) Localization of herpes simplex virus type 1 UL37 in the Golgi complex requires UL36 but not capsid structures. *J Virol* 82, 11354–61

85. Nagel, C. H., Döhner, K., Fathollahy, M., Strive, T., Borst, E. M., Messerle, M., and Sodeik, B. (2008) Nuclear egress and envelopment of herpes simplex virus capsids analyzed with dual-color fluorescence HSV1(17+). *J Virol* 82, 3109–24

86. de Oliveira, A. P., Glauser, D. L., Laimbacher, A. S., Strasser, R., Schraner, E. M., Wild, P., Ziegler, U., Breakefield, X. O., Ackermann, M., and Fraefel, C. (2008) Live visualization of herpes simplex virus type 1 compartment dynamics. *J Virol* 82, 4974–90

87. Sugimoto, K., Uema, M., Sagara, H., Tanaka, M., Sata, T., Hashimoto, Y., and Kawaguchi, Y. (2008) Simultaneous tracking of capsid, tegument, and envelope protein localization in living cells infected with triply fluorescent herpes simplex virus 1. *J Virol* 82, 5198–211

88. Desai, P., Akpa, J. C., and Person, S. (2003) Residues of VP26 of herpes simplex virus type 1 that are required for its interaction with capsids. *J Virol* 77, 391–404

89. Antinone, S. E., Shubeita, G. T., Coller, K. E., Lee, J. I., Haverlock-Moyns, S., Gross, S. P., and Smith, G. A. (2006) The Herpesvirus capsid surface protein, VP26, and the majority of the tegument proteins are dispensable for capsid transport toward the nucleus. *J Virol* 80, 5494–8

90. Desai, P., and Person, S. (1998) Incorporation of the green fluorescent protein into the herpes simplex virus type 1 capsid. *J Virol* 72, 7563–8

91. Krautwald, M., Maresch, C., Klupp, B. G., Fuchs, W., and Mettenleiter, T. C. (2008) Deletion or green fluorescent protein tagging of the pUL35 capsid component of pseudorabies virus impairs virus replication in cell culture and neuroinvasion in mice. *J Gen Virol* 89, 1346–51

92. Kobayashi, R., Kato, A., Oda, S., Koyanagi, N., Oyama, M., Kozuka-Hata, H., Arii, J., and Kawaguchi, Y. (2015) Function of the Herpes Simplex Virus 1 Small Capsid Protein VP26 Is Regulated by Phosphorylation at a Specific Site. *J Virol* 89, 6141–7

93. Radtke, K., Kieneke, D., Wolfstein, A., Michael, K., Steffen, W., Scholz, T., Karger, A., and Sodeik, B. (2010) Plus- and minus-end directed microtubule motors bind simultaneously to herpes simplex virus capsids using different inner tegument structures. *PLoS Pathog* 6, 1–20

94. Dai, X., Yu, X., Gong, H., Jiang, X., Abenes, G., Liu, H., Shivakoti, S., Britt, W. J., Zhu, H., Liu, F., and Zhou, Z. H. (2013) The smallest capsid protein mediates binding of the essential tegument protein pp150 to stabilize DNA-containing capsids in human cytomegalovirus. *PLoS Pathog* 9, e1003525

95. Dai, X., Gong, D., Xiao, Y., Wu, T.-T., Sun, R., and Zhou, Z. H. (2015) CryoEM and mutagenesis reveal that the smallest capsid protein cements and stabilizes Kaposi's sarcoma-associated herpesvirus capsid. *Proc Natl Acad Sci U S A* 112, E649–56

96. Booy, F. P., Trus, B. L., Newcomb, W. W., Brown, J. C., Conway, J. F., and Steven, A. C. (1994) Finding a needle in a haystack: detection of a small protein (the 12-kDa VP26) in a large complex (the 200-MDa capsid of herpes simplex virus). *Proc Natl Acad Sci U S A*

91, 5652–6

97. Chen, D. H., Jakana, J., McNab, D., Mitchell, J., Zhou, Z. H., Dougherty, M., Chiu, W., and Rixon, F. J. (2001) The pattern of tegument-capsid interaction in the herpes simplex virus type 1 virion is not influenced by the small hexon-associated protein VP26. *J Virol* 75, 11863–7

98. Yang, K., Wills, E., Lim, H. Y., Zhou, Z. H., and Baines, J. D. (2014) Association of herpes simplex virus pUL31 with capsid vertices and components of the capsid vertex-specific complex. *J Virol* 88, 3815–25

99. Reynolds, A. E., Ryckman, B. J., Baines, J. D., Zhou, Y., Liang, L., and Roller, R. J. (2001) U(L)31 and U(L)34 proteins of herpes simplex virus type 1 form a complex that accumulates at the nuclear rim and is required for envelopment of nucleocapsids. *J Virol* 75, 8803–17

100. Wills, E., Mou, F., and Baines, J. D. (2009) The U(L)31 and U(L)34 gene products of herpes simplex virus 1 are required for optimal localization of viral glycoproteins D and M to the inner nuclear membranes of infected cells. *J Virol* 83, 4800–9

101. Schnee, M., Ruzsics, Z., Bubeck, A., and Koszinowski, U. H. (2006) Common and specific properties of herpesvirus UL34/UL31 protein family members revealed by protein complementation assay. *J Virol* 80, 11658–66

102. Funk, C., Ott, M., Raschbichler, V., Nagel, C. H., Binz, A., Sodeik, B., Bauerfeind, R., and Bailer, S. M. (2015) The Herpes Simplex Virus Protein pUL31 Escorts Nucleocapsids to Sites of Nuclear Egress, a Process Coordinated by Its N-Terminal Domain. *PLoS Pathog* 11, e1004957

103. Hagen, C., Dent, K. C., Zeev-Ben-Mordehai, T., Grange, M., Bosse, J. B., Whittle, C.,

Klupp, B. G., Siebert, C. A., Vasishtan, D., Bäuerlein, F. J. B., Cheleski, J., Werner, S., Guttmann, P., Rehbein, S., Henzler, K., Demmerle, J., Adler, B., Koszinowski, U., Schermelleh, L., Schneider, G., Enquist, L. W., Plitzko, J. M., Mettenleiter, T. C., and Grünewald, K. (2015) Structural Basis of Vesicle Formation at the Inner Nuclear Membrane. *Cell* 163, 1692–1701

104. Zeev-Ben-Mordehai, T., Weberruß, M., Lorenz, M., Cheleski, J., Hellberg, T., Whittle, C., El Omari, K., Vasishtan, D., Dent, K. C., Harlos, K., Franzke, K., Hagen, C., Klupp, B. G., Antonin, W., Mettenleiter, T. C., and Grünewald, K. (2015) Crystal Structure of the Herpesvirus Nuclear Egress Complex Provides Insights into Inner Nuclear Membrane Remodeling. *Cell Rep* 13, 2645–52

105. Conner, J., Marsden, H., and Clements, J. B. (1994) Ribonucleotide reductase of herpesviruses. *Rev Med Virol* 4, 25–34

106. Dufour, F., Bertrand, L., Pearson, A., Grandvaux, N., and Langelier, Y. (2011) The ribonucleotide reductase R1 subunits of herpes simplex virus 1 and 2 protect cells against poly(I · C)-induced apoptosis. *J Virol* 85, 8689–701

107. Wnuk, S. F., and Robins, M. J. (2006) Ribonucleotide reductase inhibitors as anti-herpes agents. *Antiviral Res* 71, 122–6

108. Chabaud, S., Lambert, H., Sasseville, A. M. J., Lavoie, H., Guilbault, C., Massie, B., Landry, J., and Langelier, Y. (2003) The R1 subunit of herpes simplex virus ribonucleotide reductase has chaperone-like activity similar to Hsp27. *FEBS Lett* 545, 213–218

109. Langelier, Y., Bergeron, S., Chabaud, S., Lippens, J., Guilbault, C., Sasseville, A. M. J., Denis, S., Mosser, D. D., and Massie, B. (2002) The R1 subunit of herpes simplex virus

ribonucleotide reductase protects cells against apoptosis at, or upstream of, caspase-8 activation. *J Gen Virol* 83, 2779–89

110. Chabaud, S., Sasseville, A. M. J., Elahi, S. M., Caron, A., Dufour, F., Massie, B., and Langelier, Y. (2007) The ribonucleotide reductase domain of the R1 subunit of herpes simplex virus type 2 ribonucleotide reductase is essential for R1 antiapoptotic function. *J Gen Virol* 88, 384–94

111. Guo, H., Kaiser, W. J., and Mocarski, E. S. (2015) Manipulation of apoptosis and necroptosis signaling by herpesviruses. *Med Microbiol Immunol* 204, 439–48

112. Sheaffer, A. K., Newcomb, W. W., Brown, J. C., Gao, M., Weller, S. K., and Tenney, D. J. (2000) Evidence for controlled incorporation of herpes simplex virus type 1 UL26 protease into capsids. *J Virol* 74, 6838–48

113. Thomsen, D. R., Newcomb, W. W., Brown, J. C., and Homa, F. L. (1995) Assembly of the herpes simplex virus capsid: requirement for the carboxyl-terminal twenty-five amino acids of the proteins encoded by the UL26 and UL26.5 genes. *J Virol* 69, 3690–703

114. Albright, B. S., Kosinski, A., Szczepaniak, R., Cook, E. a, Stow, N. D., Conway, J. F., and Weller, S. K. (2015) The Putative Herpes Simplex Virus 1 Chaperone Protein UL32 Modulates Disulfide Bond Formation during Infection. *J Virol* 89, 443–53

115. Lyman, M. G., Feierbach, B., Curanovic, D., Bisher, M., and Enquist, L. W. (2007) Pseudorabies virus Us9 directs axonal sorting of viral capsids. *J Virol* 81, 11363–71

116. Snyder, A., Polcicova, K., and Johnson, D. C. (2008) Herpes simplex virus gE/gI and US9 proteins promote transport of both capsids and virion glycoproteins in neuronal axons. *J Virol* 82, 10613–24

117. Tomishima, M. J., and Enquist, L. W. (2001) A conserved alpha-herpesvirus protein

necessary for axonal localization of viral membrane proteins. *J Cell Biol* 154, 741–52

118. Trus, B. L., Newcomb, W. W., Cheng, N., Cardone, G., Marekov, L., Homa, F. L., Brown, J. C., and Steven, A. C. (2007) Allosteric Signaling and a Nuclear Exit Strategy: Binding of UL25/UL17 Heterodimers to DNA-Filled HSV-1 Capsids. *Mol Cell* 26, 479–489

119. Coller, K. E., Lee, J. I. H., Ueda, A., and Smith, G. A. (2007) The capsid and tegument of the alphaherpesviruses are linked by an interaction between the UL25 and VP1/2 proteins. *J Virol* 81, 11790–7

120. Kramer, T., and Enquist, L. W. (2012) Alphaherpesvirus infection disrupts mitochondrial transport in neurons. *Cell Host Microbe* 11, 504–14

121. Chowdary, T. K., Cairns, T. M., Atanasiu, D., Cohen, G. H., Eisenberg, R. J., and Heldwein, E. E. (2010) Crystal structure of the conserved herpesvirus fusion regulator complex gH-gL. *Nat Struct Mol Biol* 17, 882–8

122. Stampfer, S. D., and Heldwein, E. E. (2013) Stuck in the middle: structural insights into the role of the gH/gL heterodimer in herpesvirus entry. *Curr Opin Virol* 3, 13–9

123. Eisenberg, R. J., Atanasiu, D., Cairns, T. M., Gallagher, J. R., Krummenacher, C., and Cohen, G. H. (2012) Herpes virus fusion and entry: a story with many characters. *Viruses* 4, 800–32

124. Klupp, B. G., Granzow, H., Klopfleisch, R., Fuchs, W., Kopp, M., Lenk, M., and Mettenleiter, T. C. (2005) Functional analysis of the pseudorabies virus UL51 protein. *J Virol* 79, 3831–3840

125. Daikoku, T., Ikenoya, K., Yamada, H., Goshima, F., and Nishiyama, Y. (1998) Identification and characterization of the herpes simplex virus type 1 UL51 gene product.

J Gen Virol 79, 3027–3031

126. Lenk, M., Visser, N., and Mettenleiter, T. C. (1997) The pseudorabies virus UL51 gene product is a 30-kilodalton virion component. *J Virol* 71, 5635–5638

127. Nozawa, N., Kawaguchi, Y., Tanaka, M., Kato, A., Kato, A., Kimura, H., and Nishiyama, Y. (2005) Herpes simplex virus type 1 UL51 protein is involved in maturation and egress of virus particles. *J Virol* 79, 6947–6956

128. Roller, R. J., Haugo, A. C., Yang, K., and Baines, J. D. (2014) The Herpes Simplex Virus 1 UL51 Gene Product Has Cell Type-Specific Functions in Cell-to-Cell Spread. *J Virol* 88, 4058–68

129. Kopp, M., Granzow, H., Fuchs, W., Klupp, B., and Mettenleiter, T. C. (2004) Simultaneous deletion of pseudorabies virus tegument protein UL11 and glycoprotein M severely impairs secondary envelopment. *J Virol* 78, 3024–3034

130. Leege, T., Fuchs, W., Granzow, H., Kopp, M., Klupp, B. G., and Mettenleiter, T. C. (2009) Effects of simultaneous deletion of pUL11 and glycoprotein M on virion maturation of herpes simplex virus type 1. *J Virol* 83, 896–907

131. Meckes, D. G., and Wills, J. W. (2007) Dynamic interactions of the UL16 tegument protein with the capsid of herpes simplex virus. *J Virol* 81, 13028–13036

132. Yeh, P. C., Meckes, D. G., and Wills, J. W. (2008) Analysis of the interaction between the UL11 and UL16 tegument proteins of herpes simplex virus. *J Virol* 82, 10693–10700

133. Kopp, M., Granzow, H., Fuchs, W., Klupp, B. G., Mundt, E., Karger, A., and Mettenleiter, T. C. (2003) The pseudorabies virus UL11 protein is a virion component involved in secondary envelopment in the cytoplasm. *J Virol* 77, 5339–51

134. Loomis, J. S., Courtney, R. J., and Wills, J. W. (2003) Binding partners for the UL11

tegument protein of herpes simplex virus type 1. *J Virol* 77, 11417–11424

Figure legends:

Figure 1: Workflow procedure to generate and process protein-protein interaction data for the HVint database.

Figure 2: Circular layout of the novel PPI network. The respective node size indicates the number of interacting partners for each protein (*degree*). The edge width is scaled according to the confidence score associated with the interaction. Nodes are colour-coded according to the respective protein location in the virion particles – grey: protein has not been detected in virions by MS by Loret *et al.* 2008 (34); cyan – capsid or capsid-associated protein; orange – tegument protein; yellow – envelope glycoprotein; dark blue – other envelope protein (not glycoproteins).

Figure 3: Venn diagram showing the total number of non-redundant PPIs in the source public databases, *i.e.* IntAct (6-2015), VirHostNet (VHN; 6-2015), DIP (10-2015), BioGRID (10-2015) and PDB (6-2015). Numbers in parentheses refer to the total number of interactions originating from each source database. Numbers inside the coloured areas indicate the degree of overlap between datasets. Empty subsets indicate zero overlap.

Figure 4: (A) Venn diagram showing the total number of non-redundant PPIs in the novel HVint database classified as native and homologous interactions, respectively. The numbers in parenthesis refer to the total number of PPIs; the numbers inside the circles indicate the degree of dataset overlap. **(B)** Venn diagram showing the number of non-redundant proteins involved in PPIs in the HVint database. Proteins are involved in native and/or homologous interactions. The numbers in parenthesis refer to the number of non-redundant proteins in the respective dataset with the numbers inside the circles indicating the degree of dataset overlap.

Figure 5: Sub-network highlighting homologous PPIs with a MIscore > 0.4 in red (Supplementary table 2). The node size indicates the number of interacting partners for each

protein (*degree*). Edge width is scaled according to the confidence score associated with the PPI. The nodes are colour-coded according to the protein location in the virion particles – grey: protein has not been detected in virions by MS by Loret *et al.* (34); cyan – capsid and capsid-associated protein; orange – tegument protein; yellow – envelope glycoprotein; dark blue – envelope protein (not glycoprotein).

Figure 6: Validation of homologous PPIs by IP-MS. **(A)** Schematic of the HSV-1 (strain 17^{+}) genome indicating the locus (UL35 gene) that encodes for GFP-tagged VP26. (**B**) Experimental design for IP-MS validation of predicted VP26 protein interactions. Primary human fibroblasts were infected with HSV1 GFP or HSV1 GFPVP26, then collected and cryogenically lysed. GFPVP26 and control GFP were immuno-affinity purified from cell lysates using α-GFP antibodies conjugated to magnetic beads. Co-isolated proteins were eluted from the beads and resolved by SDS-PAGE, followed by nLC-MS/MS analysis. (**C**) Fluorescence microscopy of human foreskin fibroblasts infected with HSV1-GFPVP26. The cellular localization of GFP-tagged VP26 was visualized by direct fluorescence (green) at 14 hrs post-infection (hpi). Nuclei were stained by DAPI (blue). Scale bar = 20 μm. **(D)** The HVint sub-network of homologous predicted PPIs (Figure 5) was annotated to indicate PPIs that were co-isolated with VP26 (pUL35) by IP-MS. Both direct (red edges) and indirect, secondary (blue edges) PPIs are highlighted.

Figure 7: Novel interactions predicted by HVint and supported by IP-MS experiments (Figure 6) in the context of the viral life cycle. Proteins are colour-coded according to the protein location in the virion particles – grey: protein has not been detected in virions by MS by Loret *et al.* 2008 (34); cyan – capsid and capsid-associated protein; orange – tegument protein; yellow – envelope glycoprotein. Solid lines indicate predicted interactions in HSV-1 with MIscore > 0.4; dashed

lines indicate predicted interactions with MIscore ≤ 0.4. Both direct (red edges) and indirect, secondary (blue edges) PPIs are highlighted.

Figure 1. (Location: Experimental Procedures – Scoring of Interaction Data; Results – HVint Interactome)

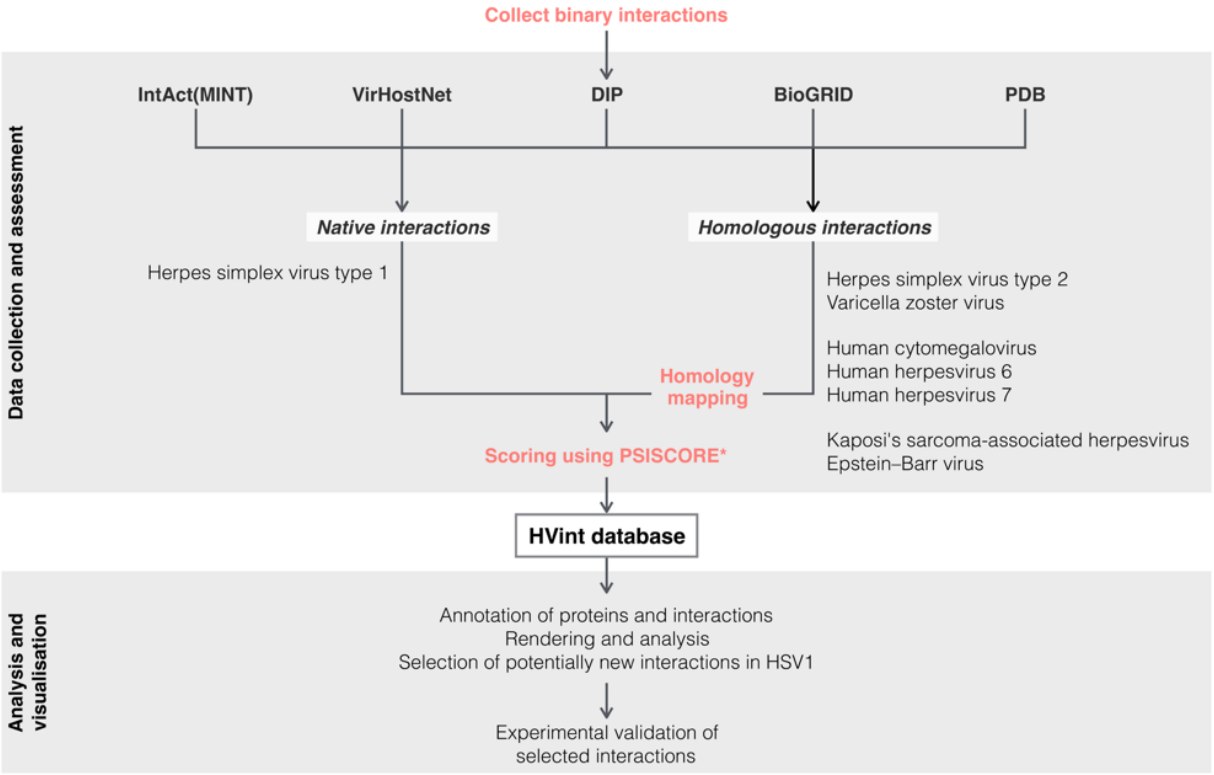

Figure 2. (Location: Results – HVint Interactome)

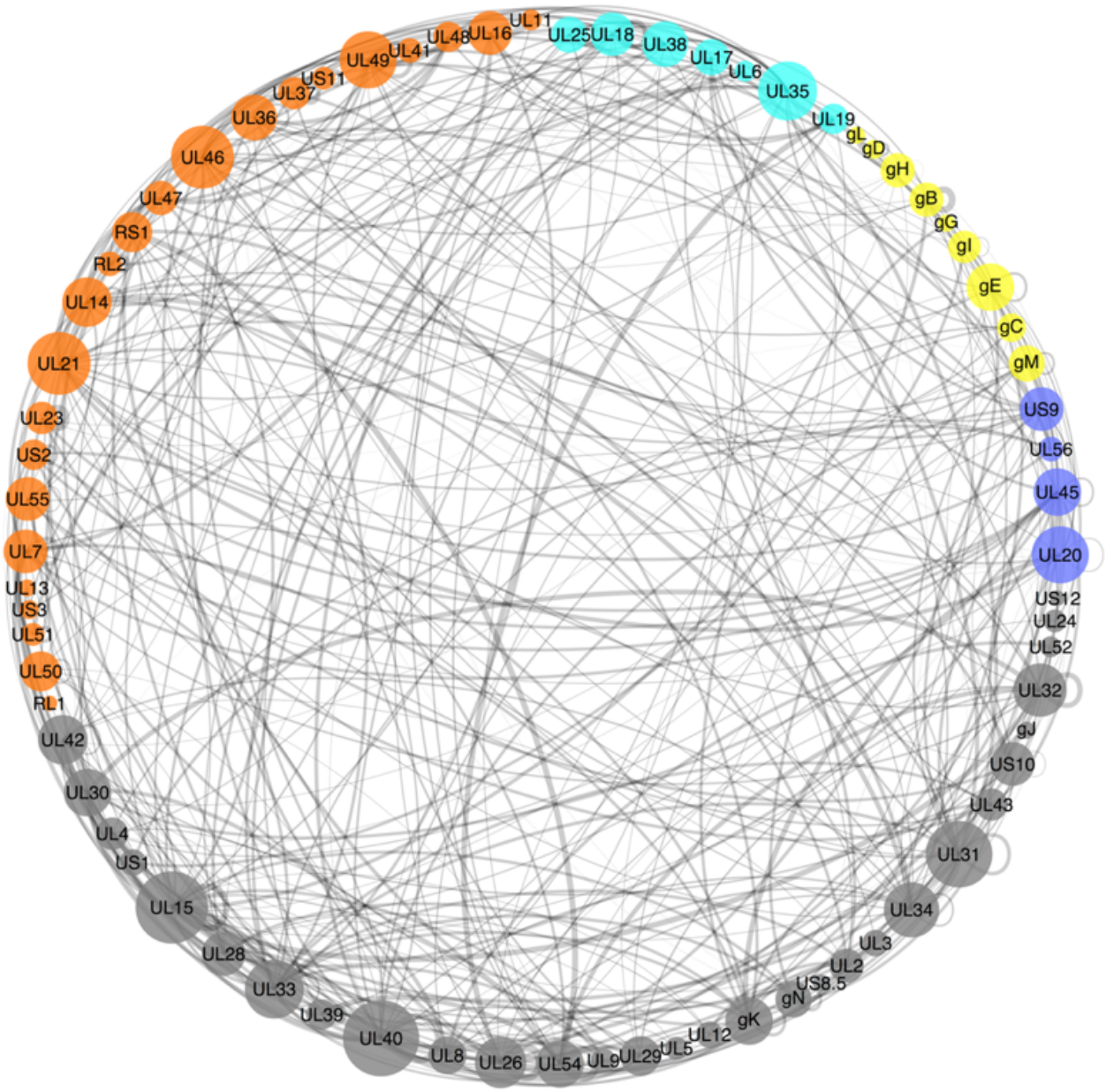

Figure 3. (Location: Results – HVint Interactome)

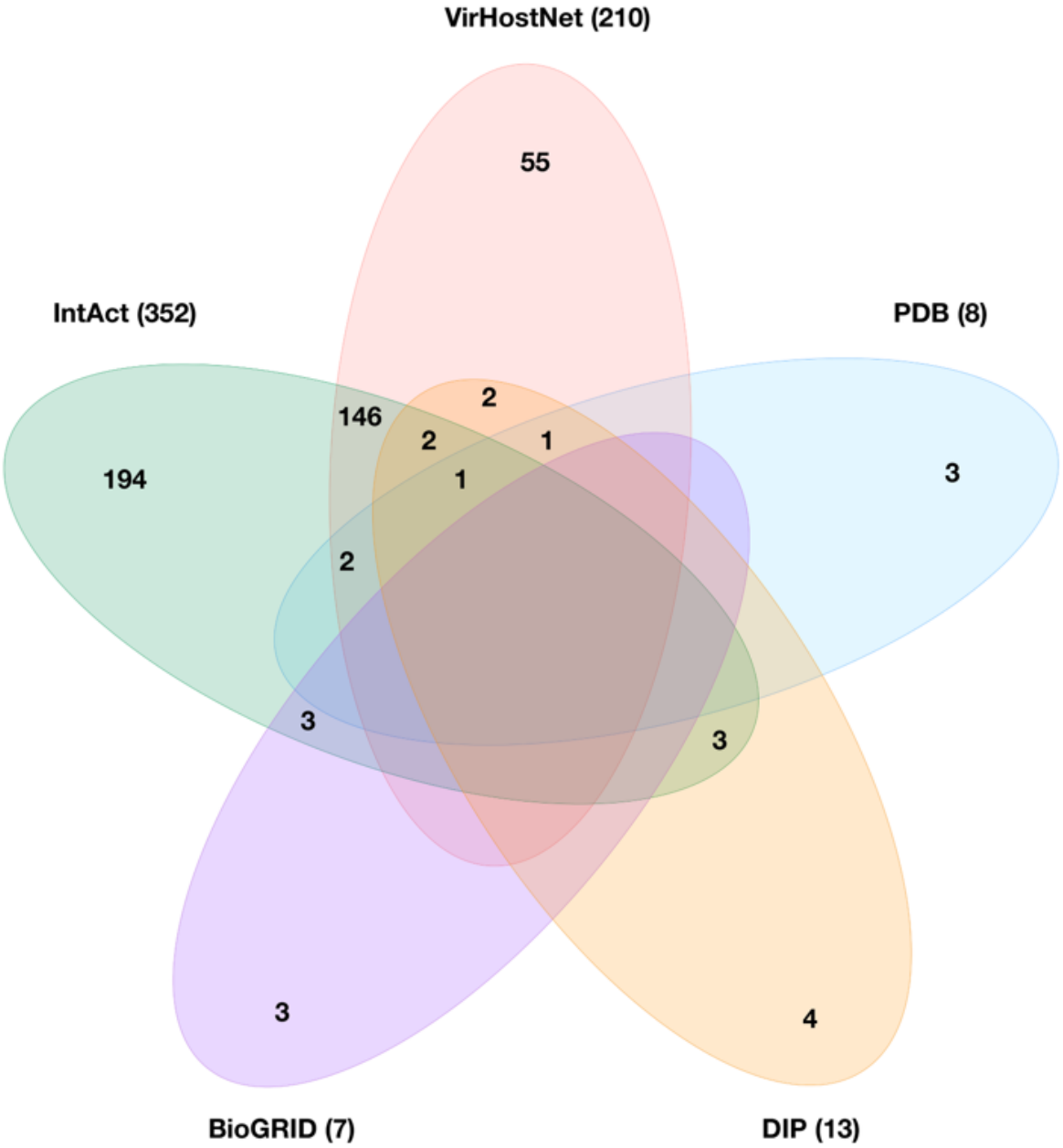

Figure 4. (Location: Results – HVint Interactome)

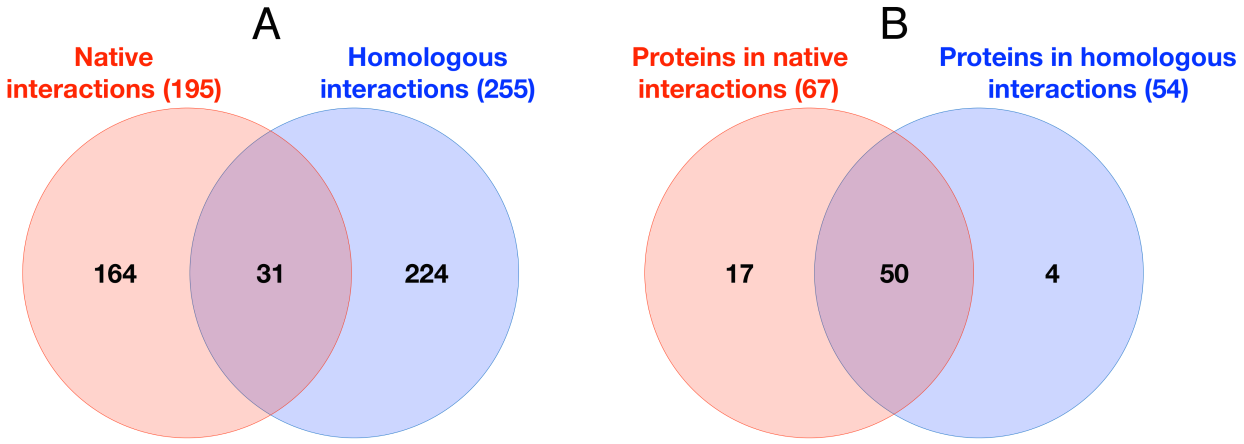

Figure 5. (Location: Results – New Interactions; Results – Validation of New Interactions)

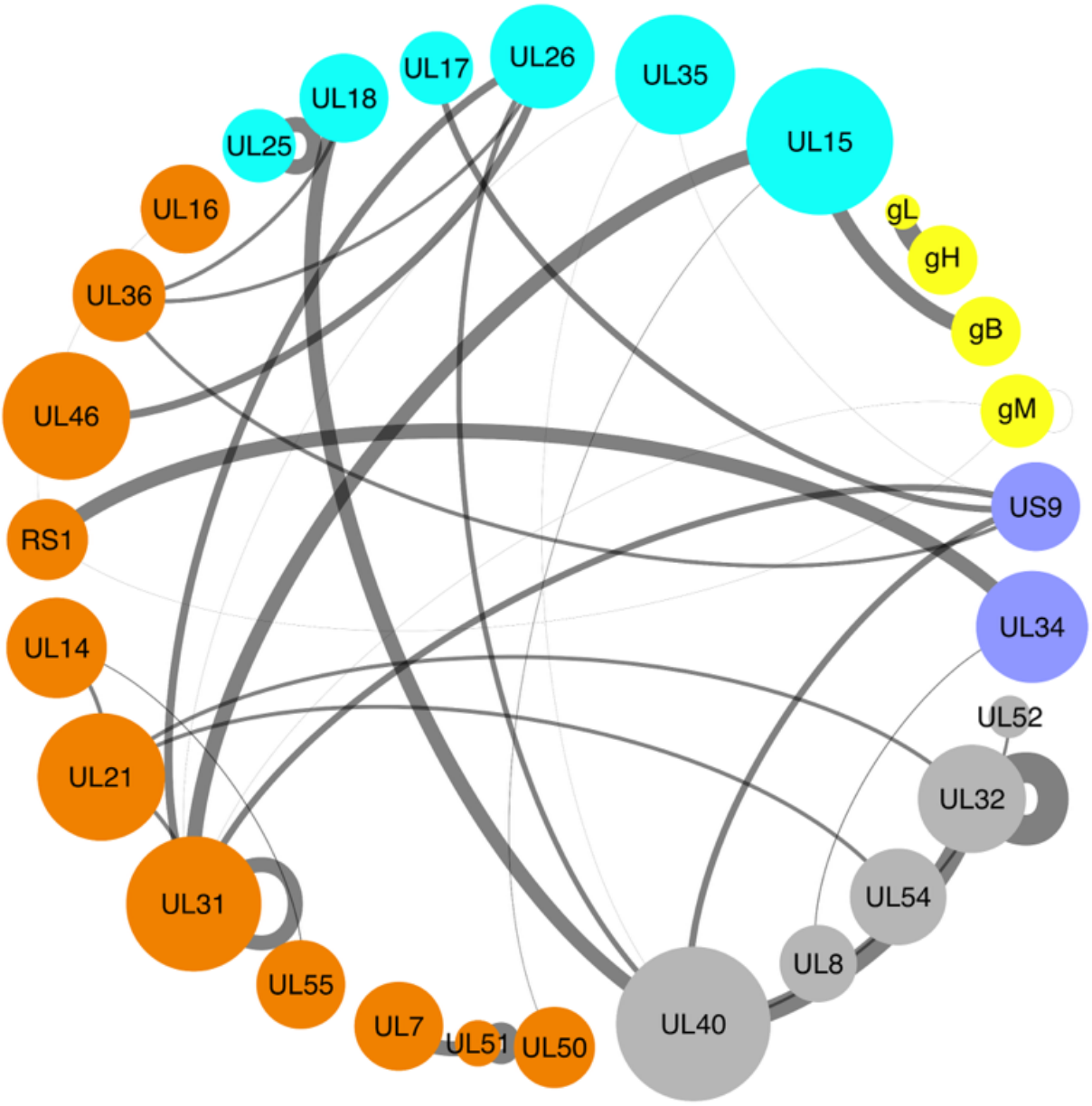

Figure 6. (Location: Results – Validation of New Interactions)

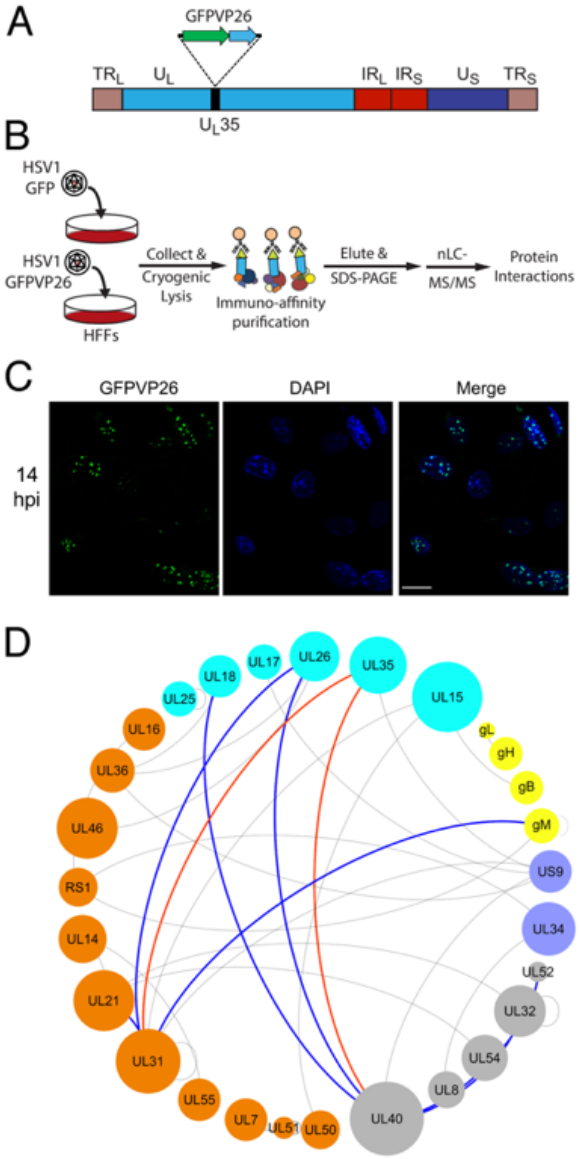

Figure 7. (Location: Discussion)